NAL PROPOSAL No. 2 B

Scientific Spokesman:
Gerald A. Smith
Physics Department
Michigan State University
East Lansing, Michigan 48823

FTS/Off-net: 517 - 372-1910
353-5180

STUDY OF MULTIPARTICLE p-p INTERACTIONS FROM 100 GeV/c to 400 GeV/c WITH A 30-INCH BUBBLE CHAMBER - OPTICAL SPARK CHAMBER HYBRID SYSTEM

R. G. Glasser, B. Kehoe, G. McLellan, W. Risk
G. A. Snow, B. Sechi-Zorn, and G. Zorn;
University of Maryland

Z. M. Ma, B. Y. Oh, G. A. Smith and R. J. Sprafka;
Michigan State University

B. Crawley, R. O. Haxby, and W. Kernan;
Iowa State University

Y. Cho, R. Engelmann, L. Voyvodic, and R. Walker;
Argonne National Laboratory

April, 1971

II. Physics Justification

We list some of the topics which will be studied in the proposed experiment and which would provide precise and much needed data to test existing models of high energy interactions.

(i) How do distributions of cross sections, prong number, transverse and longitudinal momenta vary with incident particle energy[1] in pp multiparticle reactions above 100 GeV/c? More specifically, the hypothesis of limiting fragmentation[2] and other models[3] can be tested.

A study of prong distribution will show whether σ_n, the cross section for n-prong events, approaches a finite limit as the incident momentum reaches 400 GeV/c; whether the prong distribution does satisfy a Poisson distribution as suggested by the multiperipheral and parton models; what is the energy dependence of the mean multiplicity $\langle n \rangle$?; e.g. the multiperipheral model prediction $\langle n \rangle \sim \mathrm{Ln}(s)$ would be tested over a wide energy range.

A detailed study of some single particle spectra will answer the question of whether they show limiting behavior, e.g. does

$$\frac{d^2\sigma}{dp_L dp_T^2}$$

for p, π, K... approach a limiting distribution as predicted by the limiting fragmentation hypothesis? This can be tested for primary momenta up to 400 GeV/c. Is such a distribution factorizable?, i.e.

$$\frac{d^2\sigma}{dp_L dp_T^2} \sim f(p_L)\, g(p_T)$$

and what form does $f(p_L)$ take for p, π, Λ, $\Sigma^{\pm}$?, e.g. is

$$\frac{d\sigma}{dp_L} \sim \frac{1}{p_L^{\alpha}}$$

and what value does α take? It is clearly important to extend this to as high p_L as possible. Note also that a comparison of such single particle distributions for πp and pp reactions allows a check of quark model predictions, e.g.

$$\left(\frac{d^2\sigma}{dp_L\, dp_T^2}\right)_{\pi p} \sim \frac{2}{3}\left(\frac{d^2\sigma}{dp_L\, dp_T^2}\right)_{pp}.$$

(ii) The question of whether pionization actually occurs will be much easier to decide at these high energies in contrast to the situation at presently available accelerator energies where pionization features are not clearly delineated.[1] Briefly, below 30 GeV/c both pp and πp data show a peak about zero in the pion cm longitudinal momentum distribution. However, low mass N^* resonances produced peripherally give decay pions dominantly in this region of cm momentum. Since the p_L distribution for pions from such processes will be spread over a much larger range at the higher energies, it will be considerably easier to look for pionization.

(iii) Exploiting the symmetry of the pp sytem, it will be possible to study the 4c channel $p(p\pi^+\pi^-)$, for which a cross section of $\sim$ 1 mb is expected, in some detail, e.g. Van Hove plots, Peyrou plots, Double-Regge-model.

(iv) Statistically significant measurements of the total and elastic cross sections, along with the elastic slopes, may be made up to 400 GeV/c. These may indeed represent the first set of measurements over such a large momentum interval.

(v) A search for short-lived ($\tau \sim 10^{-10}$ sec) new particles may be performed, using the bubble chamber's well known capability for this work. The sensitivity of this proposed exposure is ~6 events per microbarn.

(vi) As pointed out by Clark et al.,[4] a search for high mass boson states using the missing mass technique in the bubble chamber is feasible for masses greater than ~3 GeV. Thus we can explore the gross structures at high mass in the baryon system using the reactions $pp \to pB^{+}$.

To obtain statistically significant answers to most of the questions posed above will require several thousand multiparticle inelastic events at each of several well defined momenta. We believe this can be accomplished using a bubble chamber of conventional design in association with downstream spark chambers of modest design.

REFERENCES

1. A. R. Erwin and R. S. Panvini, papers presented at the International Conference on Expectations for Particle Reactions at the New Accelerators, University of Wisconsin, 1970; also, G. A. Smith, invited talk at the Symposium on High Energy Interactions and Multiparticle Production, Argonne National Laboratory, 1970.
2. High Energy Collisions, Ed. Yang, et al., Gordon and Breach (1969).
3. A discussion of these models may be found in the proceedings of International Conference on Expectations for Particle Reactions at the New Accelerators by J. D. Bjorken, N. Bali, and S. D. Drell, University of Wisconsin, 1970.
4. A. R. Clark, et al., NAL Summer Study, Vol. 4, 237 (1969).

III. Data Yields

With a beam of 6 particles/spill, one can expect on the average 0.6 interactions in the hydrogen and 0.3 in the upstream and downstream chamber walls per picture. For cross sections of ~20 mb for multiparticle events with 4 or more charged secondaries, about 12 percent of the pictures would have such events in a restricted hydrogen fiducial volume (12 inches). Thus, 10^5 pictures at each beam setting would provide $\sim 10^4$ multiparticle events for analysis. The topological estimates shown in Table I were obtained assuming a total cross section of 40 mb and by using cosmic ray results[1] for a primary momentum around 200 GeV/c.

TABLE I - Expected Yields Of Multiparticle p-p Events At 200 GeV/c For 10^5 Pictures With 6 Tracks Per Picture In 12-inches of LH_2.

TYPE	CROSS-SECTION (mb)	NO. EVENTS (Per 10^5 Pictures)
Total	40	24,000
Elastic	10	6,000
Inelastic	30	18,000
4 Prongs	6.0	3,600
6 Prongs	6.0	3,600
8 Prongs	3.8	2,300
10 Prongs	2.4	1,400
12 Prongs	1.7	1,000
14 Prongs	0.7	500
16 Prongs	0.2	100
≥ 4	20.8	12,500

It is our intention to photograph every expansion of the bubble chamber. Consequently, many interactions will be recorded on film, independent of whether additional data has been recorded by the downstream spectrometer, described in section IV. We may then proceed to rapidly analyze the film for several of the items of interest discussed in section II. For example, total cross sections,prong distributions, elastic scattering and some features of the target fragmentation may be rather quickly determined. Of course, the search for short-lived particles will be a very exciting aspect of this part of the experiment.

REFERENCES

1. L. W. Jones, in Proceedings of International Conference on Expectations for Particle Reactions at the New Accelerators, University of Wisconsin (1970).

IV. Experimental Arrangement for the Proposed 30-inch Bubble Chamber - Optical Spark Chamber Hybrid System

The main components of the proposed detector system are shown in Figure 1. These include:

(1) The 30-inch hydrogen bubble chamber, for observation of the interaction vertex and analysis of all low energy charged particles with momenta below ~20 GeV/c.

(2) An upstream beam diagnostic system for providing precise measurements of beam particles (not necessary for proton running).

(3) A wide gap optical spark chamber spectrometer situated downstream for providing important additional data on energetic secondary charged particles with momenta above approximately 20 GeV/c.

(4) A shower spark chamber system situated behind the spectrometer for information on very energetic gamma rays.

While the arrangement is similar in some respects to the bubble chamber - spark chamber detector system described in the Aspen study of Fields, et al.[1], it is not required for the present initial experiment to have the very high accuracy requirements for final state fitting which was of primary interest in the latter study.

These components are matched to the kinematic requirements, as discussed below, in such a way that they provide relatively complete examination of individual multiparticle interactions in the 100 GeV/c region and above. The most noticeable feature of multiparticle interactions as presently known is the tendency for the emitted particles to be produced with relatively small transverse momenta. Those going backwards in the cm system with large longi-

tudinal momenta then appear in the laboratory system with low momenta and large angles. Particles with small longitudinal momenta can appear in the lab at intermediate momenta and angles, while the forward particles in the cm appear as highly collimated, energetic components of a forward jet.

Examples of kinematically allowed regions for transverse and longitudinal cm momenta are shown in the Peyrou plot of Figure 2 for the case of 500 GeV/c pp interactions. Superposed are the expected contours for laboratory angles and momenta of outgoing pions, showing the characteristics described above. For greater detail, the region of small transverse momenta is shown in Figure 3. Backward pions in the cm with transverse momenta below 1 GeV/c are seen to have laboratory momenta of less than $\sim$20 GeV/c, and can appear at angles even beyond 90°.

Similar behavior is illustrated for secondary protons from 200 GeV/c pp interactions in Figure 4, except that the allowed maximum laboratory angle here must be less than 90°. On the other hand, those particles produced with small or forward longitudinal momenta P_L, and transverse momenta $P_T \lesssim 1$ GeV/c, are seen to have laboratory momenta above approximately 20 GeV/c and are confined to a forward cone of less than approximately ±4° opening angle.

1. Bubble Chamber

The main bubble chamber requirements here are good track resolution, angular precision $\lesssim$ 1 mrad, good momentum accuracy up to the 20 GeV/c region, and provision of suitable exit windows and magnet apertures for the forward secondaries. The 30-inch bubble chamber is eminently suitable, without requiring any significant modifications.

The gross chamber features illustrated in Figure 1 are those of the 30-inch, whose characteristics include high resolution dark field optics, a

magnetic field of 32 Kg, multipulsing capabilities of $\lesssim$ five expansions per 0.5 seconds, and a maximum detectable momentum of over 1000 GeV/c. In the configuration shown in Figure 1, the beam is brought in through a small window which is currently in use as an exit window for a neutral hadron hybrid spectrometer at ANL. The limiting exit angle allowed by the magnet structure in the horizontal plane is confined to approximately ±3.5°, which corresponds to allowing all secondary particles above ∿20 GeV/c to enter the downstream spark chamber spectrometer. In the vertical plane the magnet iron and beam exit windows allow particles at angles up to approximately ±10°. Thus, it is obvious that the anlysis of tracks below ∿20 GeV/c will necessarily be performed in the bubble chamber, where $\Delta p/p \lesssim 10\%$ and $\Delta\theta \lesssim 1$ mrad. This, in our opinion, is a satisfactory level of performance for this particular group of produced particles.

2. Bubble Chamber Beam

We assume that the beam to the 30-inch bubble chamber described in the Lach-Pruss report[2] will be constructed. Using the secondary hadron target, proton beams with π^+ contamination < 1% are achieveable at all requested momenta. The angular divergence required is $\sim 10^{-4}$ rad, which can be accomplished by limiting acceptance and use of a 10 mil high target. A spill time of ∿ 60-200 μ sec is assumed, with two or three such spills per accelerator pulse being highly desirable for bubble chamber multipulsing. We assume that beam tuning detectors (scintillators or wire proportional chambers) will exist and also at least one Cerenkov counter to determine relative fractions of π^+, K^+, and p. A flux-limiting fast kicker would permit much more efficient use of the bubble chamber, giving cleaner pictures and avoiding unusable pictures, and would be highly desirable.

However, since the spectrometer facility is planned to be of general use, a more comprehensive beam system would be required for beam particles other than protons. This section discusses beam characteristics and beam defining equipment which we regard as necessary to do a variety of experiments in the 30-inch bubble chamber with the associated downstream spectrometer. The additional requirements are:

A) A flux of $\sim 10^{10}$ protons at the secondary hadron target.[2]

B) A Cerenkov counter which can efficiently tag π's vs. (K and p) up to 200 GeV/c for beam purity in view of possible significant fractions of K^- and $\bar{p}$[2,3].

C) A second Cerenkov counter which can tag (π^-, K^-) vs. $\bar{p}$ will permit studies of K^- and $\bar{p}$ interactions as a by-product of a π^- experiment. Eventually K^- and $\bar{p}$ enrichment triggering might be done. If K^+/p and π^+/p ratios are good, similar arguments will apply for positive beams.

D) Position tagging of each beam track in the chamber, in time correlation with the above Cerenkov signals.

E) External determination of beam momentum and angles will be mandatory in most cases. Five small proportional wire chambers can do this job and also tag all beam tracks in (D).

The beam kicker and details of B) through E) are discussed in some detail in appendix I. Provided the beam divergence and flux can be made appropriate, however, none of these additions is necessary for proton running.

3.&4. Spark Chamber Spectrometer

Although many of the salient features of multiparticle interactions will be obtained from the analysis of only the low energy particles seen in the bubble chamber, as illustrated in the previous discussion, we believe that additional insight can be provided by supplementary information on the more energetic downstream components of the same events. The following deals with four important aspects of the system:

(A) spectrometer resolution,

(B) spark chamber optics,

(C) gamma-ray detection and,

(D) trigger schemes.

(A) Spark Chamber Spectrometer Resolution

The apparatus, as shown in Figure 1, includes no external magnetic field other than that of the bubble chamber itself. Calculations show that utilizing (a) the event vertex location in the bubble chamber (b) the chamber's fringing field and (c) track locations in the wide gap chambers a typical $\Delta p/p$ accuracy of ± 5-10% or less is readily obtainable for fast secondaries produced in a 200 GeV/c collision on hydrogen. It is clear, however, that considerable additional accuracy is available on the very small angle fast secondaries with the addition of a magnet downstream. Preliminary considerations for such a system are also presented.

In the initial scheme, two spark chamber units are utilized, one immediately behind the bubble chamber magnet with four gaps of active volume 36" wide by 48" high by 8" deep and the other unit 4.5 meters downstream, against

the far wall of the bubble chamber building, with the same dimensions. The downstream 36" dimension subtends a ±3.5° angle from the bubble chamber. Assuming the following parameters: (1) ±500 μ on each point measured in the spark chambers (2) eight points measured per spark chamber unit (3) ±100 μ on the vertex in the bubble chamber and (4) 872 Kg-in of integral Bdl in the bubble chamber fringing field we find that $\pm\Delta p/p$ (%) $\tilde{=}$ 0.07 p (GeV/c). Taking into account the following sources of error due to multiple coulomb scattering: (1) 15" of LH_2 (2) 0.12" of Fe (B.C. window) (3) 0.25" of Al (vacuum tank windows) and (4) 0.5 cm of counters and other smaller sources (air, chamber walls), the resultant $\pm\Delta p/p$(%) has been determined and is shown in Figure 5. With the exception of the fastest secondaries produced at the highest momenta proposed, the calculations show that the downstream spectrometer will provide data comparable in accuracy to that of the bubble chamber at lower secondary momenta and permit a complete study, in conjunction with the bubble chamber, of all interesting production angles.

A possible straight forward extension of the apparatus to yield more precision in the momentum determination of fast forward particles requires an additional spark chamber module plus a magnet. This would involve a large aperture magnet (e.g., an ANL type BM 109 with a 8" x 24" x 72" aperture and maximum integral Bdl of 1366 Kg-in) placed immediately downstream of the second spark chamber module followed by a third spark chamber module 5 meters from the magnet. All tracks with lab momentum $\gtrsim$ 100 GeV/c and with transverse momentum $\leq$ 1 GeV/c will be transmitted through the aperture of the magnet and will be recorded in the third spark chamber module. The deflection in the magnet, coupled with the long lever arm, provides a $\pm\Delta p/p \tilde{=}$ .012 p (%). Thus, 6-7% $\pm\Delta p/p$ or less can be achieved for all tracks of interest without altering the initial set up of the experiment, but merely extending it.

(B) Spark Chamber Optics

The wide gap chambers have an active volume 8" deep x 48" high x 36" wide per cell. Each chamber consists of 2 cells and each module consists of 2 chambers, as seen in Figure 6. The chambers are mounted on a precision platform which has three primary functions: 1) Providing a means of determining the relative locations of the two chamber modules and the bubble chamber, 2) Providing a means of maintaining a continuous check on these positions and 3) Providing a simple means of re-installing the apparatus in the beam line after removal. Measuring of apparatus locations is done by means of two theadolites, one to determine and monitor bubble chamber-spark chamber platform positions and the second to determine and monitor spark chamber-spark chamber platform positions. Leveling legs on the chambers, top, bottom, front, and rear fiducials on the chamber frame and fiducials on the precision platform serve to position the chambers in a known orientation. Front and top fiducials also appear on each film frame to orient the chambers on the film. Rear and bottom fiducials on periodically run"fiducial runs"serve to complete a three dimensional co-ordinate system for track reconstruction independent of knowledge of camera position. Additional platform fiducials in view of the camera can serve as an extra check on spark chamber-platform orientations.

The chamber separation is variable within and between modules. Within the module a maximum separation of 32" is allowed. As seen in Figure 7, this maximum separation still permits viewing both chambers in a module with one 35 mm. camera at a demagnification of 64:1. This demagnification is an upper limit permitted by the intrinsic resolution of a film such as Kodak Shellburst for a real space position accuracy of 0.1 mm. With a 4" lens

the camera can be located at 20 ft. from the center of the chambers. The chambers are inclined 6° relative to the beam line to permit a direct view in each chamber, thereby eliminating lenses and mirrors in that view (see Figure 8). The chamber windows are made of 10 mil. clear Mylar to eliminate distortions there. One precision mirror is used in the 90° stereo view to bring that view to the same camera. A fiducial plane with many fiducials is located at the bottom of the spark chamber to permit corrections due to any distortions in the mirror. 90° stereo is used for maximum accuracy in reconstruction. The direct view is the view of the plane of bend for maximum accuracy in momentum determination. A strip mirror subtending $\sim$ 1/3 of the gap in the direct view provides 10° stereo for resolving ambiguities in track reconstruction. The mirror subtends only part of one gap in each chamber to eliminate confusion between the direct and 10° stereo tracks. A dark room under slight over pressure surrounds each assembly for photographic and hydrogen safety reasons.

(C) Gamma-Ray Detection

The insertion of several radiation lengths of material between the second and third gaps of the spark chamber units will provide an effective converter for gamma-rays from fast, forward π°'s. From the point of interaction, probably measureable to $\lesssim$ 5 mm, both the frequency and direction of fast π°'s can be inferred. To our knowledge, the only previous measurement of π° frequency is that of Elbert et al.[4] at 25 GeV/c for $\pi^- p$ in a hydrogen bubble chamber with plates. Their results, although somewhat weak statistically, are in rather strong disagreement with the multiperipheral model. Clearly, more precise measurements at NAL energies will be very valuable in our proposed studies.

(D) Trigger Schemes

The trigger arrangement will be designed such that the spark chambers fire on virtually all interactions, there being nearly one per beam burst. A picture of the bubble chamber will be taken for each expansion. Two simple and flexible schemes have been devised:

(1) Energy-Loss Trigger: Referring to Figure 1, multiparticle-charge-particle secondaries would be selected by pulse-height criteria in the counters S_3 S_4 S_5. More than one particle will, on the average, give a greater pulse height than that for a single beam particle. Although one might consider almost any type of counter which gives signals proportional to the number of particles which transverse it, e.g. Cerenkov, scintillation, etc., the most simple to utilize is the scintillation counter and it also turns out to result in the thinnest detector (in g/cm^2). A single scintillation counter when traversed by a high energy particle will give a Landau pulse-height distribution. This distribution, with its long tail at high pulse heights, cannot be avoided in the present application. A pulse height of 2 times the minimum value will occur on traversal by a single minimum ionizing particle ~5% of the time. This can be greatly improved, however, if two or more counters S_1, S_2; S_3 $S_4 \ldots S_n$ are utilized and the minimum pulse height appearing is considered. In this case, the width of the distribution will be decreased by $1/\sqrt{n}$ and even for n = 3, the tail has all but vanished. If this signal is to be used to trigger the downstream chambers, the minimum pulse height must be determined in <1 μ sec.

With this method, it is to be noted that the downstream counters should be thin in order that nuclear interactions in them do not occur frequently. Such interactions are no different in character from those in the chamber and

walls and triggers due to them would certainly result. The number of these should be much smaller than those which occur in the chamber. In 1 mm of plastic scintillator a minimum ionizing particle produces $\sim 10^3$ photons. With an efficient photo cathode ($\sim$25%) and a light collection efficiency of $\sim$20%, 50 photo-electrons could result. This number is sufficient to assure that statistical fluxtuations will be relatively small. The five counters, S_1, S_2, S_3, S_4, and S_5, would represent a total thickness of 0.5 cm which is 0.5cm/52cm = 1/100 of a geometrical-mean-free-path. Thus, with 6 particles per picutre and with the counters described, in $\sim$ 6% of the pulses would the spark chamber system have recorded interactions occuring in the triggering counters $S_1S_2S_3S_4$and S_5.

For reasons of efficient and uniform light collection the size of these counters probably should not exceed 8" x 8". This presents some minor limitations in the detection of secondaries as they must appear within a cone of $\pm 3°$ if placed at a distance of $\sim$ 2 meters from the interaction. It may be possible to locate counters nearer the chamber inside the iron yoke, and if so the acceptance angle would be increased. This setup is very inefficient for elastic scattering and processes of the type $pp \rightarrow ppn(\pi^\circ)$, when the struck proton is slow and at a large angle, thus missing $S_3S_4S_5$. However, an alternate scheme, discussed next, would substantially resolve this shortcoming.

(2) Beam-Deflection Trigger: The trigger consists of a 3.0 inch diameter scintillator S_3 located in the beam 125 feet downstream from the

bubble chamber (see Figure 1). When this scintillator fails to record a particle previously observed by counters S_1, S_2 in the beam upstream of the bubble chamber, it is considered to have interacted.

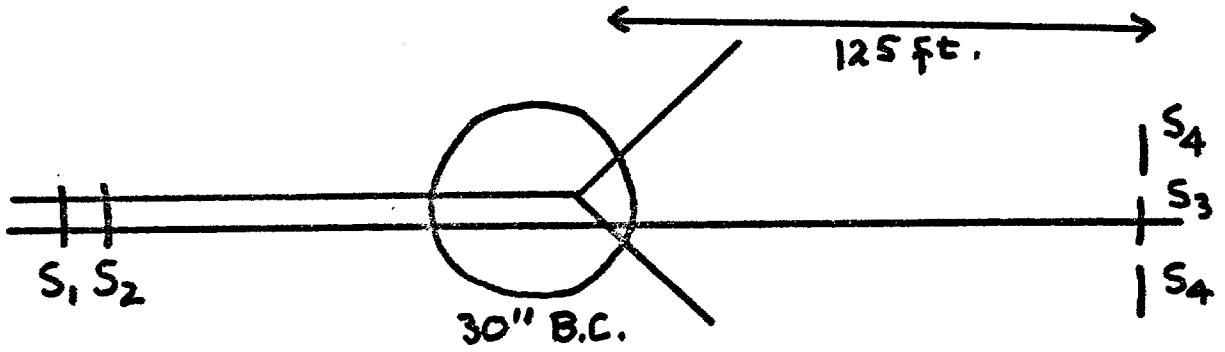

For the purposes of investigating the properties of the trigger we assume a 2.0" diameter beam in the bubble chamber. This allows a beam spread which does not diverge after leaving the chamber except for multiple Coulomb scattering. For beam momenta between 100 and 500 GeV/c the beam size at the downstream scintillator should not exceed 2.25 inches due to multiple scattering.

This trigger fails most frequently in detecting elastic scatters. Table II below lists the average minimum scatter angle and recoil range for elastic events which will actuate the trigger.

TABLE II - Minimum Angle and Recoil Range For Elastic Events

Beam Momentum GeV/c	Minimum Scatter Angle mr.	Minimum Recoil Range cm
100	1	0.3
200	1	3.5
300	1	15.0
500	1	100

There is considerable flexibility here. For example, by moving S_3 to 200 feet downstream of the bubble chamber and using a diameter of 2.5"

instead of 3.0", one achieves a minimum angle of 0.5 mr. and a minimum range of 8.0 cm at 500 GeV/c.

Some fraction of the inelastic events might also be expected to put a particle through S_3, invalidating the trigger. Scaling 25 GeV/c events to NAL energies indicates this is not very important, in part because the bubble chamber field imparts transverse momentum to a track which is several times that of the minimum detectable elastic scatter. For example at 200 GeV/c this trigger fails on 4.5% of the 2-prongs, 3% of the 4-prongs, 1% of the 6-prongs and 0.3% of the 8-prongs.[5]

This small loss of inelastic events can be reduced somewhat by surrounding S_3 with a larger counter S_4. A hole in S_4 passes beam particles on to S_3. A multiparticle accidental through S_3 is likely to be accompanied by one or more particles through S_4. Hence one would trigger on $(S_1.S_2.\overline{S_3}.S_4)$, $(S_1.S_2.\overline{S_3}.\overline{S_4})$, $(S_1.S_2.S_3.S_4)$. One can reduce the loss rate arbitrarily by increasing the size of S_4 or moving it closer to the bubble chamber.

S_3 was not placed more than 125 feet downstream of the bubble chamber so that transit time of the particles and signals would be short enough to allow adequate time to perform logical operations and apply spark chamber voltages in less than 500 ns. This restriction is probably too strict by at least a factor of two and can probably be relaxed to observe smaller angle elastic scatters. It is possible that we may prefer a beam profile in the chamber more like 5" x 1/2". In this case S_3 would be about 6.5" x 1". This has approximately the same solid angle as the circular counter discussed above and presents no focusing problems for the presently planned beam.

Finally, it is emphasized that both these triggers are flexible and most certainly can be studied quickly and efficiently under test beam conditions. It would be our intention to do so before proceeding with "Production" data-taking.

REFERENCES

1. T. H. Fields, et al., NAL Summer Study, Vol. 3, 227 (1968).
2. "Hadron Beams in the Neutrino Area", J. Lach and S. Pruss, NAL Report TM-285, 2254.000.
3. "Extrapolated Ratios of K^- and $\bar{p}$ to π^- from High Energy Protons on Aluminum Measured at Serpukhov," V. E. Barnes, Purdue University High Energy Physics Note # 313, April 1, 1971.
4. J. W. Elbert et al., Nuclear Physics B19, 85 (1970).
5. A. Erwin, University of Wisconsin (private communication).

V. Apparatus and Obligations

The apparatus has been thoroughly discussed in the previous sections. The cost and construction of the entire system downstream of the bubble chamber will be assumed by the Maryland - MSU - ISU - ANL collaboration.

It is assumed that NAL will provide an operating, track - sensitive bubble chamber staffed with a crew plus film (three-view, 35 mm format). It is imperative that a thorough magnetic field map be performed, preferably before the start of the run. Members of the collaboration will gladly participate, although it is preferred that NAL provide the necessary equipment.

It appears certain that, pending approval of this proposal, the entire downstream apparatus could be ready for test studies in a beam by the nominal turn-on date of the chamber, November 1, 1971. We estimate that one month of beam studies will render the apparatus ready for "production" data-taking.

For the second half of the proposed experiment, the collaboration will request from NAL a BM 109 type magnet.

FIGURE CAPTIONS

Fig. 1 Components of the proposed hybrid system.

Fig. 2 Contours of laboratory angle and momentum on the Peyrou Plot for the π in the reaction $p + p \rightarrow \pi^+ + \ldots$ at 500 GeV/c.

Fig. 3 Shows more detail of Fig. 2.

Fig. 4 Detail of contours of laboratory angle and momentum on the Peyrou Plot for the proton in the reaction $p + p \rightarrow p + \ldots$ at 200 GeV/c.

Fig. 5 Calculated momentum resolution for the apparatus of Fig. 1.

Fig. 6 Wide gap optical spark chamber (one of two such chambers).

Fig. 7 Wide gap optical spark chambers and camera positioning.

Fig. 8 Format of images on 35 mm film.

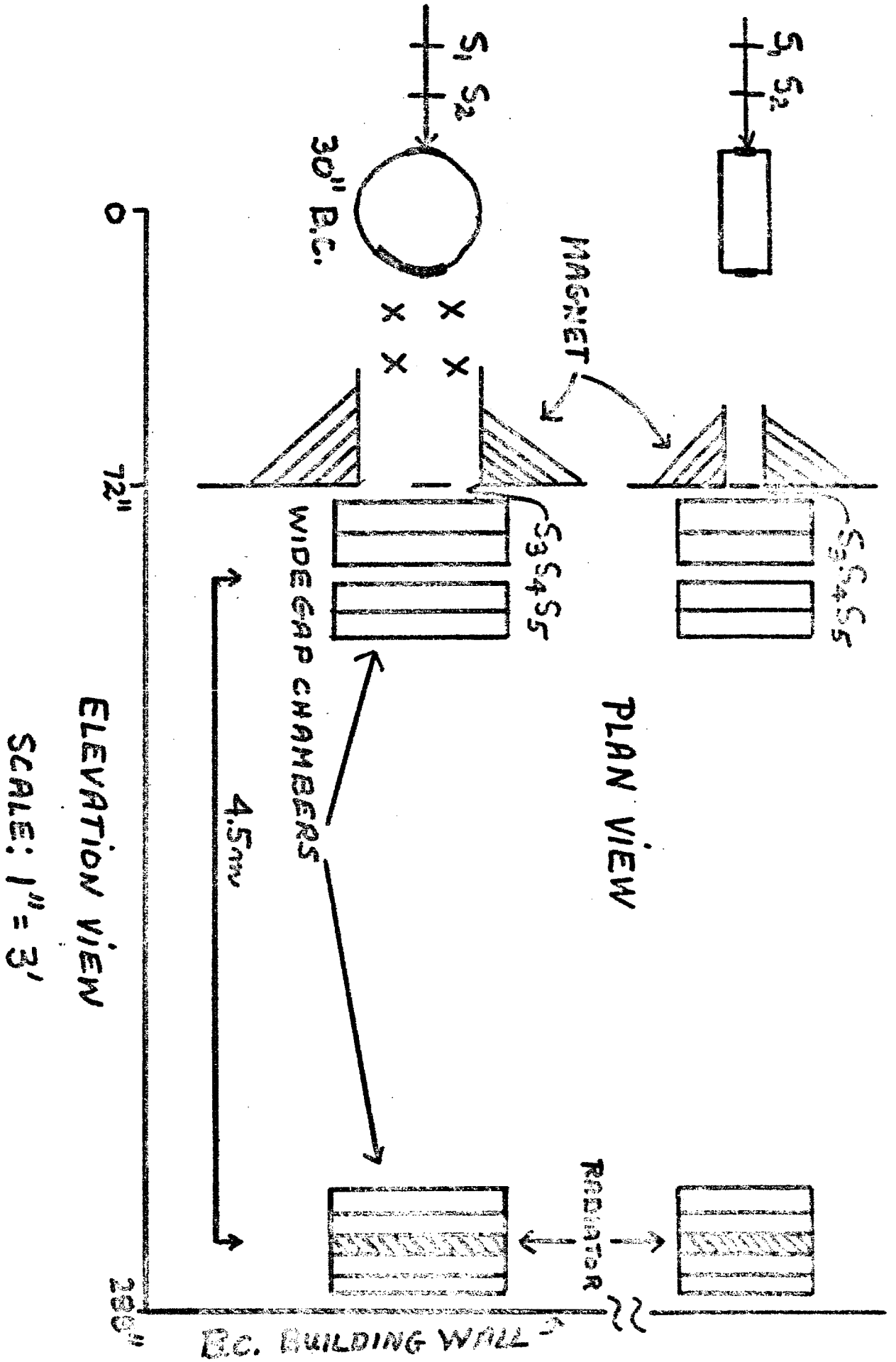
S1 S2
30" D.C.
S1 S2
MAGNET
0
72"
WIDE GAP CHAMBERS
S3 S4 S5
S3 S4 S5
4.5"w
PLAN VIEW
ELEVATION VIEW
SCALE: 1" = 3'
RADIATOR
288"
D.C. BUILDING WALL

FIGURE 1

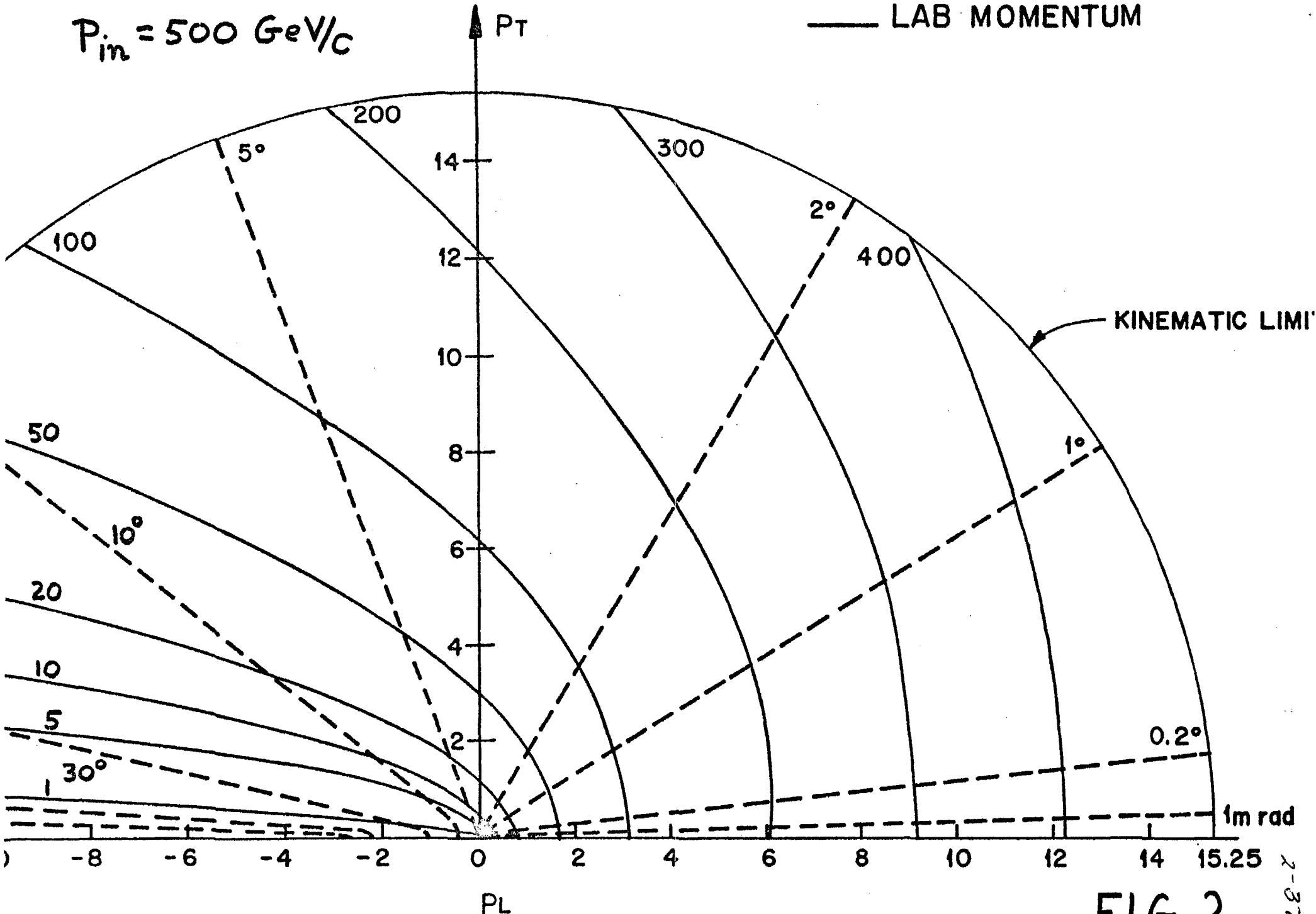
p-p → π+ ·····
P_in = 500 GeV/c
---LAB ANGLE
——— LAB MOMENTUM
PT
PL
100
200
300
400
50
20
10
5
1
5°
2°
1°
0.2°
10°
30°
1m rad
KINEMATIC LIMI
14
12
10
8
6
4
2
-8
-6
-4
-2
0
2
4
6
8
10
12
14
15.25

FIG. 2

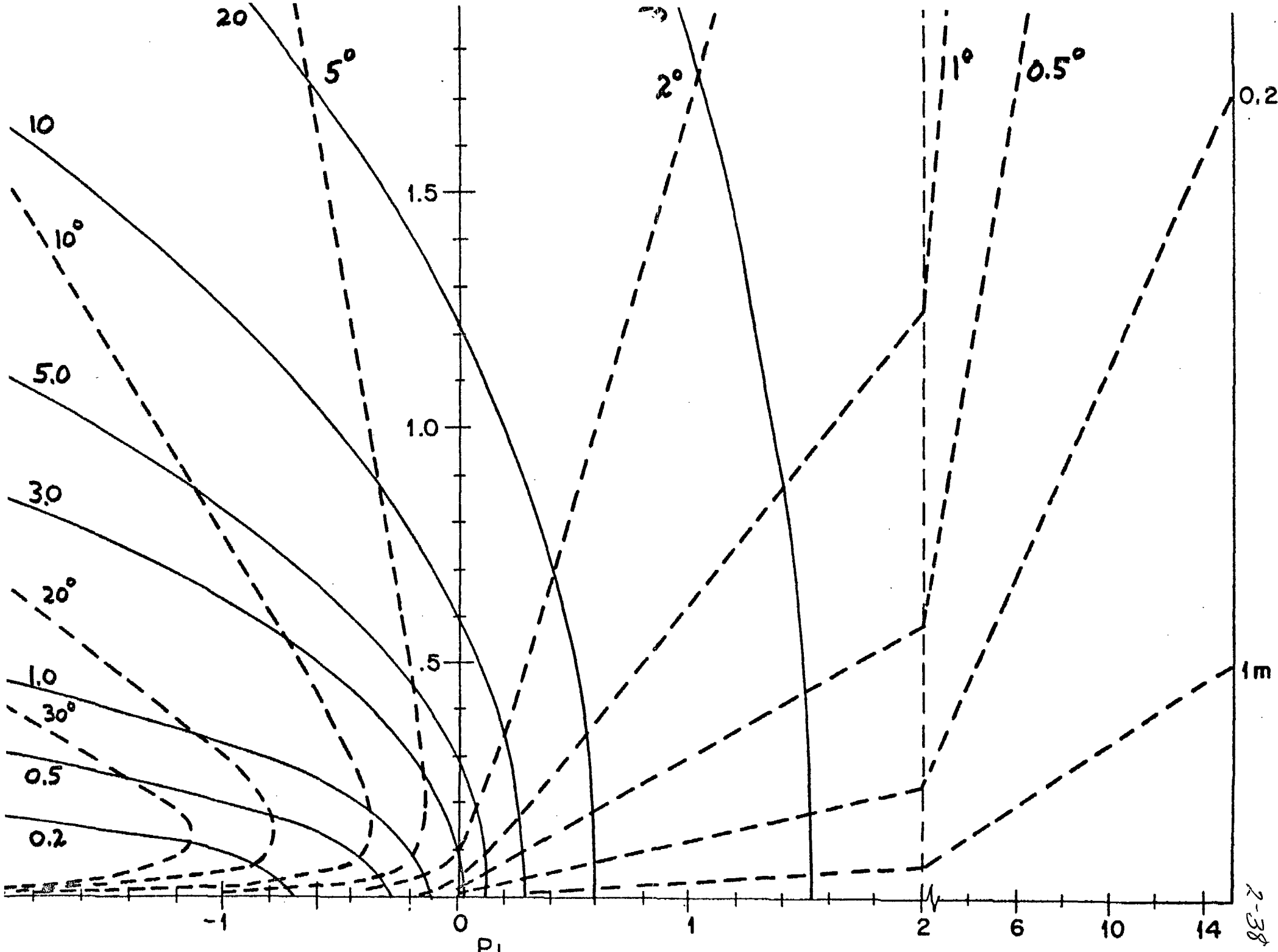

FIG. 3

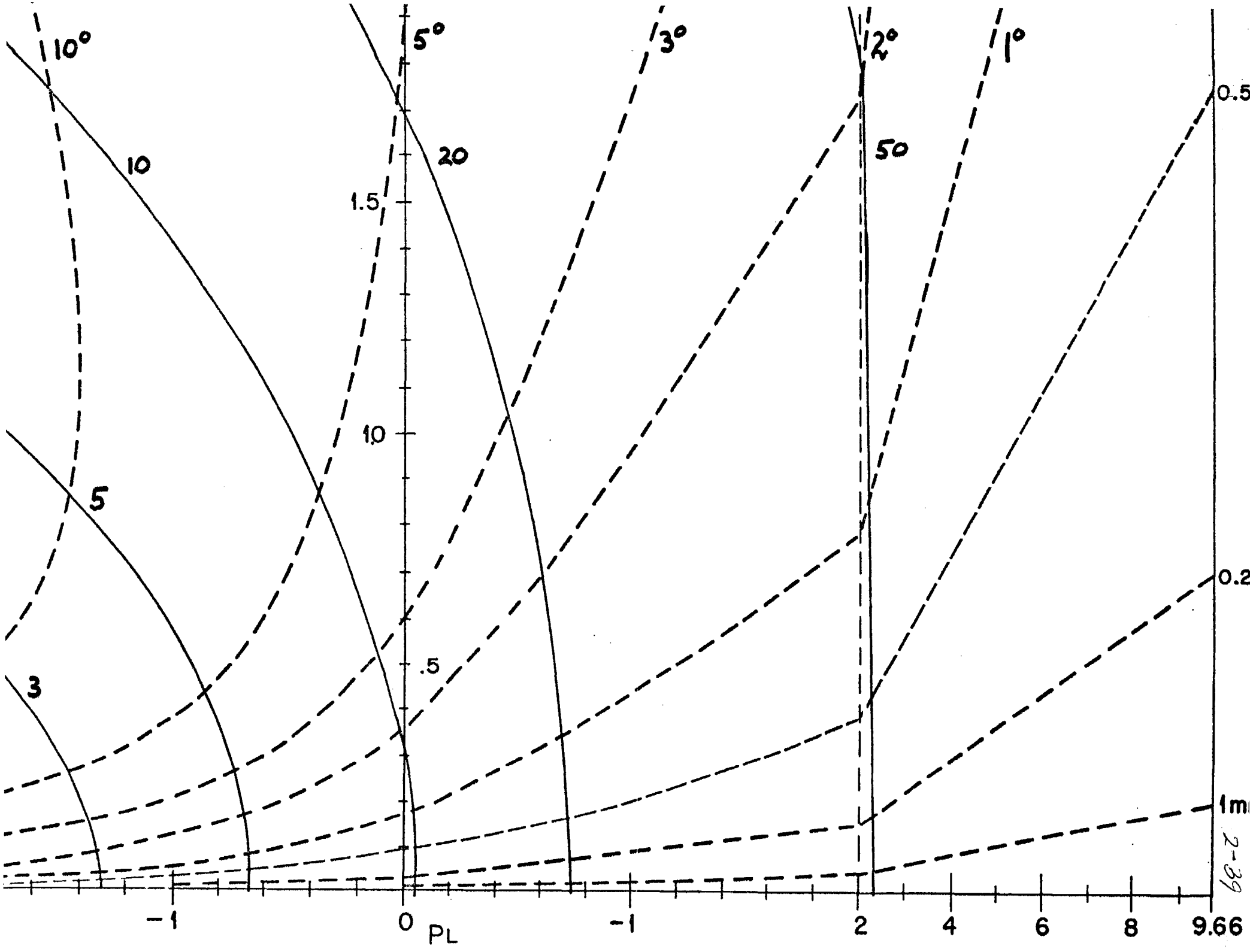

FIG. 4

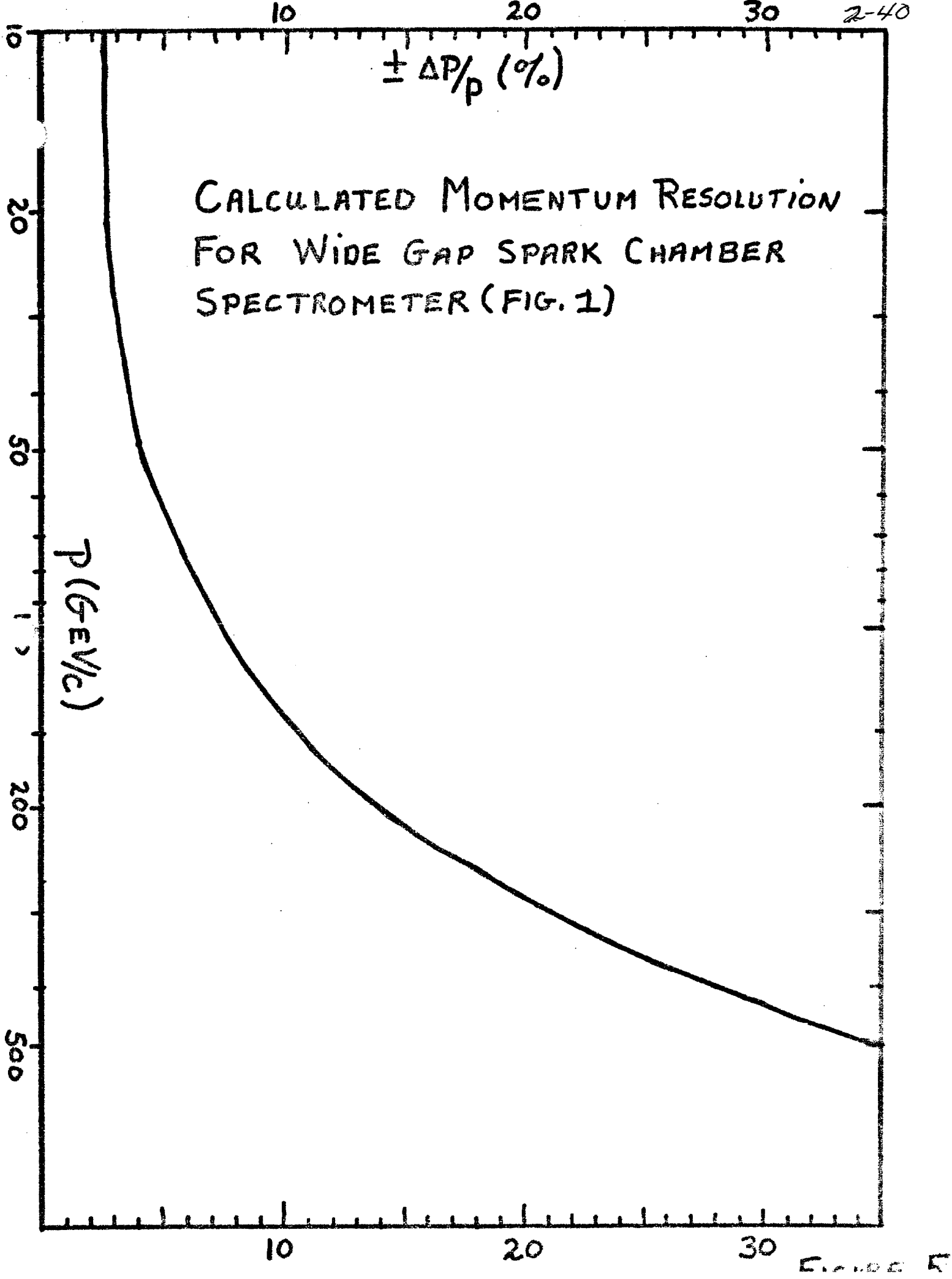
10
20
30
± ΔP/p (%)
CALCULATED MOMENTUM RESOLUTION
FOR WIDE GAP SPARK CHAMBER
SPECTROMETER (FIG. 1)
P (GEV/c)
1
2
5
10
20
50
100
200
500
10
20
30

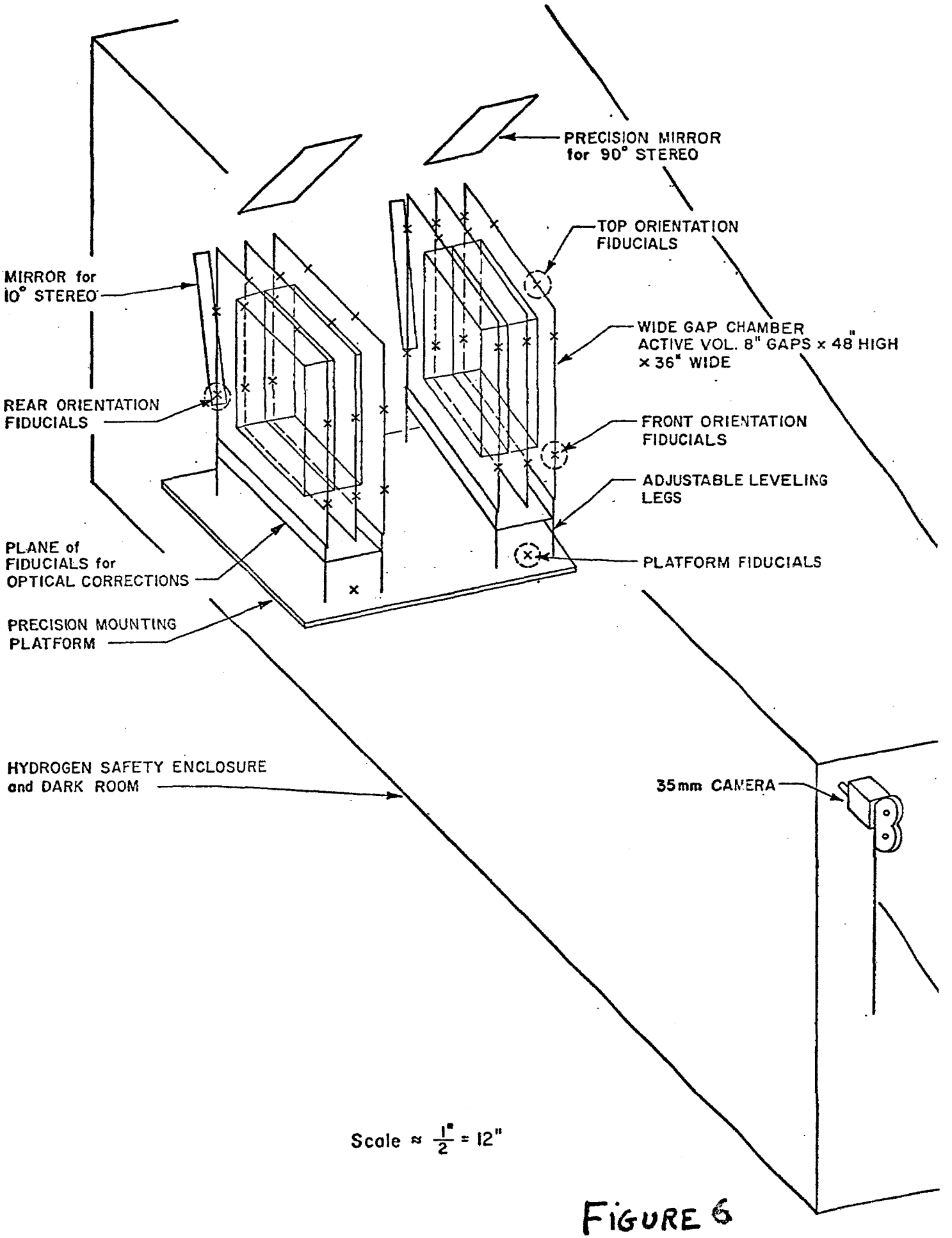

Scale ≈ $\frac{1}{2}$" = 12"

FIGURE 6

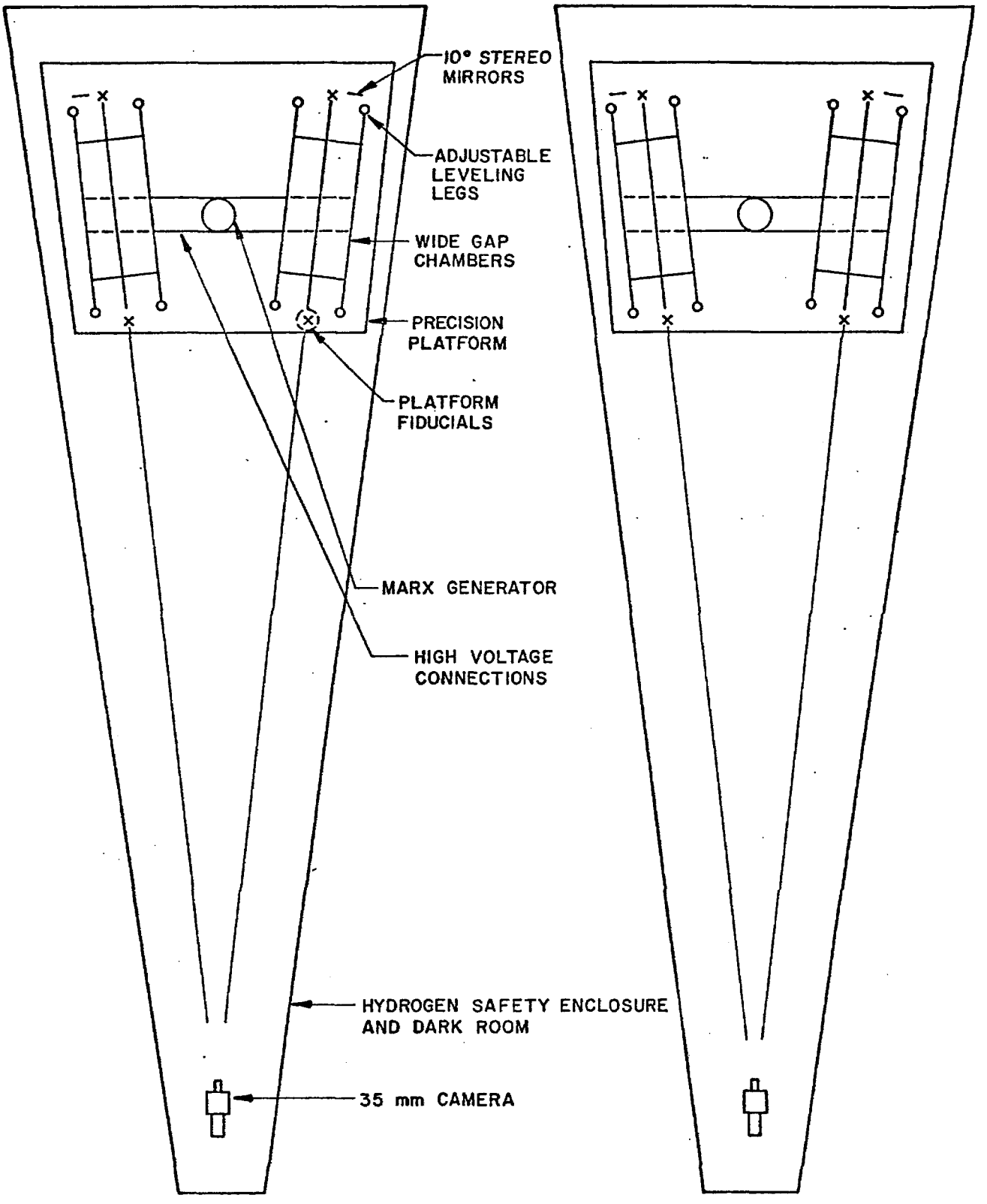

PLAN VIEW
SCALE ≈ $\frac{1}{2}$" = 12"

FIGURE 7

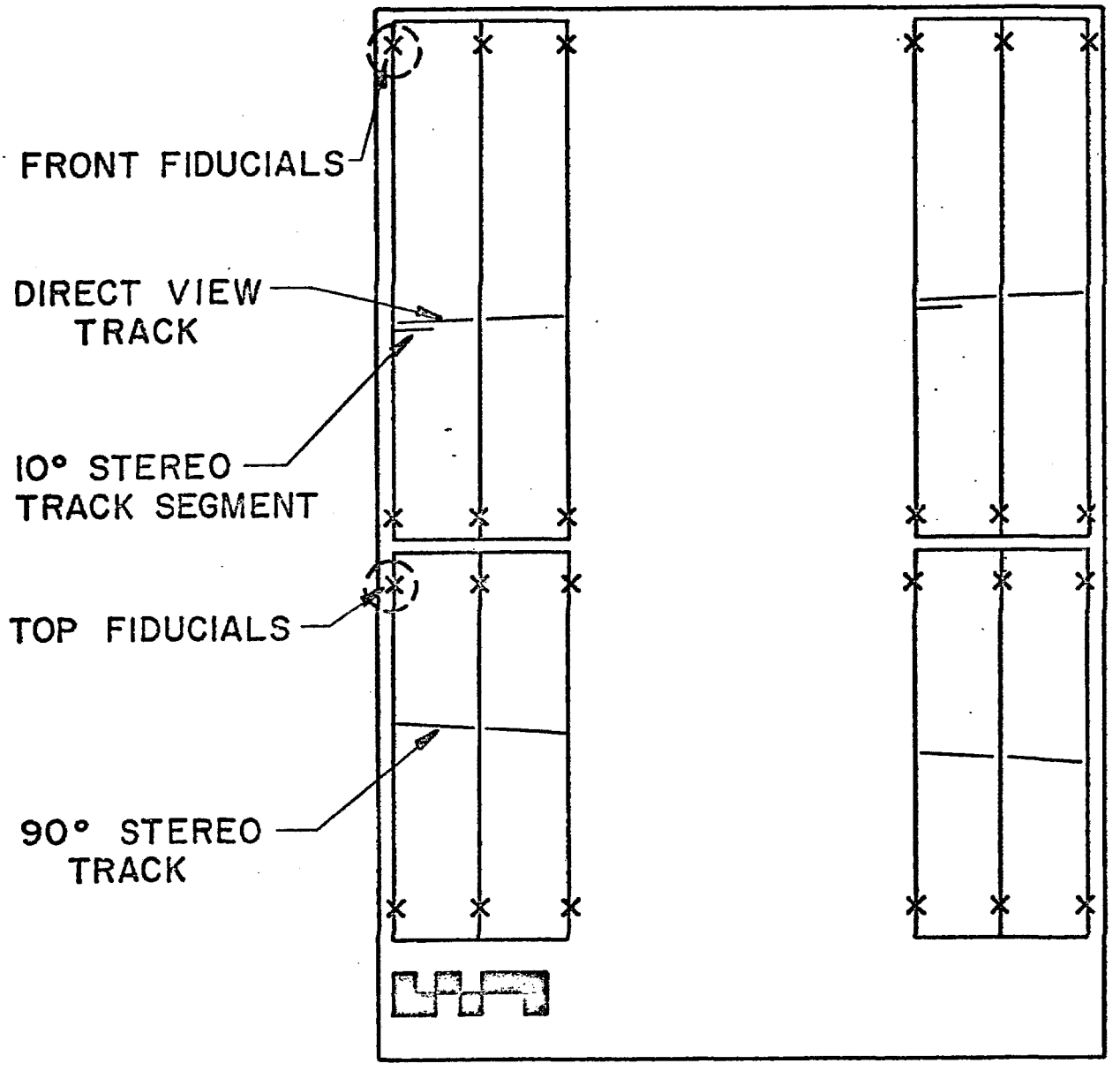

FILM FORMAT 35 mm 1.5" × 1.0"

FIGURE 8

Appendix I.

Here we include some detailed suggestions to make the hybrid spectrometer a more useful, flexible facility.

A) Fast Flux Limiting Beam Kicker

A 1-2 μ sec. kicker with integral $Bdl \tilde{=}$ one Kg-m would kick the 5mm high target image upward by 0.065 mrad, or by 13 mm with a 200 meter lever arm. The kicker should be located 1000 feet from the chamber. However, the beam track counter should be placed at the chamber entry window to avoid uncertainty in the track count. The signal propagation delay (~2 μ sec.) is comparable to the rise time, plus there are logic and ignition delays. Given a total delay of 4 to 7 μ sec., n = 10 tracks/picture, and 100 μ sec. spill time, one should be able to control the flux to ± 2 tracks. This is enormously better than the typical fluctuations without a kicker, and should eliminate a source of wasted bubble chamber photographs and wasted accelerator pulses.

B and C) Cerenkov Tagging of π, K and p

Extrapolations[1] of Serpukhov data indicate that 500 GeV/c protons on a target will produce a rich ratio of K^-/π^- and $\bar{p}/\pi^-$ at 100 GeV/c -- 5% and 15% respectively, 1 km. away at the bubble chamber. The need for π^- tagging in this case is obvious, and the opportunity to study tagged K^- and $\bar{p}$ interactions early is attractive. In secondary positive beams, p and π^+ and probably K^+ will all be present in significant amounts at some energies, and will require tagging.

S. Pruss (NAL) has suggested a differential Cerenkov design, an outgrowth of ideas he presented at the 1970 Summer Study.[2] Small angle light is directed to one phototube and light between this angle and a larger angle

is directed to a second phototube. For Cerenkov angles ∿5 mrad, the angular separation of π's from K's at 200 GeV/c is several times the natural beam divergence of 0.1 mrad, or the chromatic $\Delta\theta$. Good photon fluxes at these angles should permit efficient tagging at $p \lesssim$ 200-250 GeV/c or beyond. A second Cerenkov counter of identical design would then permit separation of p from K and π.

The design involves 40m of Helium-filled pipe at ∿.2 to 1 atmosphere absolute, downstream diameter 12" to 18", a 100" focal length spherical mirror, and the above-mentioned phototube array. High counting efficiencies can be obtained even beyond 200 GeV/c in the differential mode of operation with this length. Beam divergence must be $\lesssim$ 0.1 mrad, close to what is achievable in the existing beam design.[3] Pressure must be monitored to 10 mm of mercury and average temperatures to 5°C.

D) Position Tagging of Tracks to Correlate with Cerenkov Information

Minimal position tagging could be accomplished with a crossed pair of picket fence scintillator arrays. This means a non-negligible number of photomultiplier tubes, -- since the number of x-y resolution elements should be many times greater than the number of beam tracks to reduce the probability of two tracks in one hodoscope location. Moreover, one must record the bubble chamber frame number and x-y for each beam track. Thus, a fast parallel shift register is needed to absorb information during the beam spill and later pass it on to a computer or perhaps directly to an incremental tape unit.

With this in mind, the use of small proportional wire arrays of 50 to 100 wires, read out as above, appears attractive. One gets greater x-y resolution at somewhat less cost and can also achieve the purposes of item (E). Such a system is illustrated in Figure 1.

E) Angle and Momentum Tagging

To use the 30" bubble chamber efficiently, one should start the fiducial volume immediately at the beginning of the liquid. Hence, one must know p and θ of the beam externally. In any case, one can do better externally than by measuring short beam tracks in the liquid. From beam optics one will have $\delta\theta \simeq 10^{-4}$ rad and $\delta p/p = 0.066\%$.[2] However, in flux-limited situations one may want to increase the momentum bite to 1%. Then it pays to replace the momentum slit with a proportional wire array and win back the $\delta p/p$ inherent in the target size. This corresponds to a wire spacing of 2mm. A more refined system can be made with 1 mm. wire spacing, but several such chambers would be required to determine orbits better. In effect, the equivalent of a second plane near the target is needed to reduce the "target size". In this case one also improves upon the .066% which can be achieved with momentum slits.

The phase space of the beam as designed is 10^{-9} inch^2-steradian. With a reasonable beam size in the chamber, for example $\sim$ 0.5 x 3.0 inches, either the beam is parallel to 10^{-4} rad or its angle can be determined to 10^{-4} by measuring position in the chambers. This matches $\delta\theta_{coulomb} \leq 10^{-4}$ from the entry windows, and also matches for beam up to 500 GeV/c with the transverse momentum accuracy one obtains from measuring outgoing tracks in the last half of the bubble chamber or better still in the wide gap optical chambers.

To survey the proportional chambers, a well measured non-interacting track in the bubble chamber determines θ to 0.5×10^{-4} in y, and 1.5×10^{-4} in z, while $\delta\theta(coulomb)\sim10^{-4}$ from the entry windows. At a distance of 13 m, the wire location is known to 1.5 and 2.4 mm respectively in y and z, from a single track.

The use of an existing, tested design of Charpak chamber[4] with good space resolution and immunity to spark chamber noise, compact and with a relatively small number of wires in total, appears attractive. One could certainly put the information onto magnetic tape, together with Cerenkov counter signals, for each beam track into the bubble chamber. Frame numbers would also be written onto the tape between beam pulses. A small computer would be the most flexible readout device. A fast parallel shift register or equivalent will be needed to interface the proportional wire and Cerenkov signals. The computer could in principle be dispensed with and the information written directly from the shift register by an incremental tape unit, but with the loss of online diagnostic capabilities. Given a computer with a fast printer, the track tagging information could be printed out frame by frame for each roll, avoiding magnetic tape and associated format problems for the user.

REFERENCES

1. "Extrapolated Ratios of K^- and $\bar{p}$ to π^- from High Energy Protons on Aluminum Measured At Serpukhov," V. E. Barnes, Purdue University High Energy Physics Note # 313, April 1, 1971.
2. S. Pruss, NAL Summer Study (1970), p. 103.
3. "Hadron Beams in the Neutrino Area," J. Lach and S. Pruss, NAL Report TM-285, 2254.000.
4. M. Atac and J. Lach, Nucl. Instr. and Methods 86 (1970), p. 173.

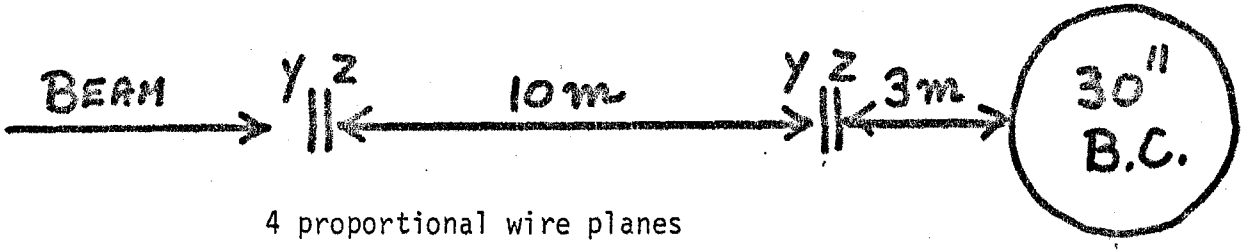

4 proportional wire planes

1 mm wire spacing

2"x2", 50 wires. This can be scaled up by a factor 2 in y if needed.

The momentum defining proportional chamber is not shown, being over 1000' upstream at a focus where the image of the target is ∿2 mm in size. The dispersion is ∿2 "/% at this point.

FIGURE 1